PROCEEDINGS OF SCIENCE

Improving the sensitivity of KM3NeT to MeV-GeV neutrinos from solar flares

Jonathan Mauro[a,*] **and Gwenhaël de Wasseige**[a] **on behalf of the KM3NeT Collaboration**

[a] *Centre for Cosmology, Particle Physics and Phenomenology - CP3, Universite Catholique de Louvain, B-1348 Louvain-la-Neuve, Belgium*

E-mail: jonathan.mauro@uclouvain.be, gwenhael.dewasseige.@uclouvain.be

The detection of MeV-GeV neutrinos from astronomical sources is a long-lasting challenge for neutrino experiments. The low flux predicted for transient sources, such as solar flares, and their low-energy signature, requires a detector with both a large instrumented volume as well as a high density of photomultiplier tubes (PMTs). We discuss how KM3NeT can play a key role in the search for these neutrinos. KM3NeT is a Cherenkov neutrino telescope currently under deployment, located at the bottom of the Mediterranean Sea. It consists of two arrays of Digital Optical Modules (DOMs): KM3NeT/ORCA and KM3NeT/ARCA, which are optimised for the detection of GeV neutrinos for oscillation studies, and higher-energy astronomical neutrinos respectively. We exploit the multi-PMT configuration of KM3NeT's DOMs to develop the techniques that allow the disentangling of the MeV-GeV neutrino signature from the atmospheric and environmental background. Comparing data with neutrino simulations we identify the variables with discriminating power, and by applying hard cuts we are able to reject a large fraction of background. We present a graph neural network approach to classify signal from background. To further improve the sensitivities compared to previous studies, we will make use of the Hierarchical Graph Pooling with Structure Learning algorithm and will use graph-structured data to reproduce the hit geometry on the DOM. This will allow for stronger constraints on the hits and reduce the fraction of background that survives the selection.

38th International Cosmic Ray Conference (ICRC2023)
26 July - 3 August, 2023
Nagoya, Japan

*Speaker

PoS(ICRC2023)1294

1. Introduction

KM3NeT is a neutrino telescope currently operating at the bottom of the Mediterranean Sea. It consits of an array of Detection Units (DUs), to each of which are attached 18 Digital Optical Modules (DOMs), which contain 31 photomultipliers tubes (PMTs) each. These are used to detect the Cherenkov light emitted from charged particles originating from interactions of neutrinos with the sea water [1]. KM3NeT consists of two separate blocks: KM3NeT/ORCA, which is located in the South of France near Toulon, and is optimised to detect GeV neutrinos, and KM3NeT/ARCA, which is close to Capo Passero in Sicily, and more sensitive to neutrinos with energies between several tens of GeV to PeV. The detector is currently under deployment, and it is going to result in an instrumented volume of about 1 cubic kilometre for KM3NeT/ARCA and $3.6 \times 10^6 \mathrm{m}^3$ for KM3NeT/ORCA.

Although the main objective of KM3NeT is to investigate neutrinos in the multiple-GeV to TeV energy range, its large volume and relative high-density of instrumentation present a unique opportunity to study transient neutrino sources, such as solar flares, at sub-GeV energies. The current sensitivity of KM3NeT to astrophysical sources in the few-GeV energy range comes from the modified Neutrino-Mass-Ordering (NMO) selection in KM3NeT/ORCA, which is described in [2]. However, this selection still relies on multi-DOM coincidences, thus it's not optimal to investigate sub-GeV neutrinos as they are not expected to trigger multiple DOMs.

For neutrinos with energies of a few MeV, an event selection that uses coincidences at the single-DOM level has been implemented in KM3NeT [3]. This is mainly used to investigate Core Collapse Supernovae (CCSN), and it demonstrates the potential of KM3NeT to resolve low-energy signatures thanks to its unique DOM design. The CCSN neutrino flux is however expected to be high at energies well below the GeV, and the dedicated selection is then not well suited to probe lower fluxes at higher energies.

In its rawest form, KM3NeT data contains groups of two or more PMT-hits recorded in coincidence of 10 ns on the same DOM. Each hit has an associated time and time-over-treshold (ToT), where ToT is the duration of the pulse above approximately 0.3 photo-electrons, and can loosely be interpreted as a charge measurement. This type of data is referred to as L1, it is dominated by coincidences caused by decay of ^{40}K, naturally present in sea water, while other major contributions come from bioluminescent species and atmospheric muons [1].

Solar flares are extremely energetic events that occur in the solar atmosphere, they are observed as peaks in the gamma-ray flux and/or in the X-ray flux, and they are often associated with other interesting phenomena, such as Coronal Mass Ejections (CMEs) and production of Solar Energetic Particles (SEPs), i.e., high-energy charged particles. These observations describe solar flares as sites of particle acceleration, and therefore, as perfect candidates to be neutrino sources. Moreover, there is most likely a link between gamma rays and neutrinos, as discussed in [4]: gamma-ray observations and spectral analysis prove pion production to happen in the most energetic solar flares, implying that flares with a strong gamma-ray flux should have an associated neutrino flux in the MeV-GeV range, as a result of pion decay.

Estimates of the solar-flare neutrino flux can be found in the literature, we refer the interested reader to some notable examples [4–6]. Solar-flare neutrino flux predictions are inferred by estimating the accelerated proton's energy fraction that goes into pion production. As such predictions

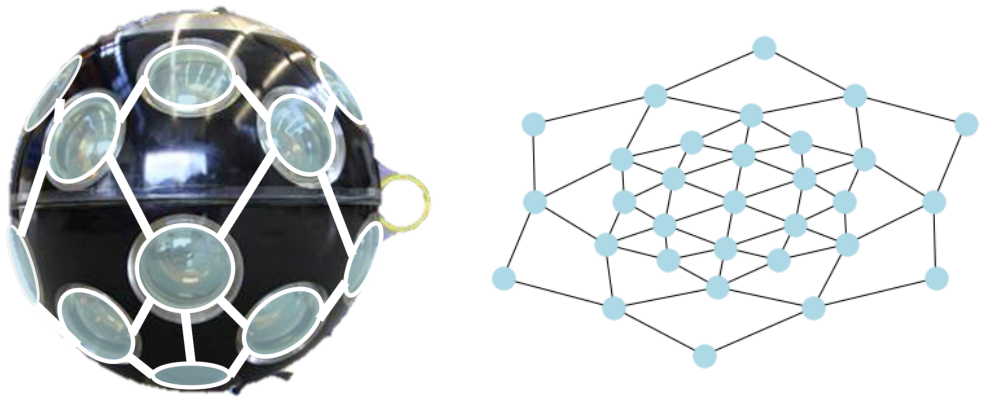

(a) (b)

Figure 1: (a) DOM-graph superimposed on a picture of a KM3NeT DOM. (b) DOM-graph as represented by NetworkX's graphic tools.

are highly dependent on the assumptions made on the accelerated proton's beam, and on the sun's density profile, there are significant differences between the proposed models. We highlight that the optimistic prediction of Fargion's model [6] has the expected neutrino flux almost within the sensitivities of current neutrino telescopes, and strict constraints have already been set by IceCube in the high energy range [7], and by Super-Kamiokande at lower energies [8]. Being able to cover a broad energy range, KM3NeT will be the ideal instrument to further constrain neutrino production in solar flares.

While machine learning has been largely implemented in all applications of particle physics, recently graph neural networks (GNNs) have caught the attention of the experimental neutrino physics community as well. The reason for this is that the architecture of the detectors, and thus the structure of the data, can be naturally encoded into graphs by exploiting the spatial and temporal relations between the hits recorded by multiple PMTs. In this context GNNs can be used for regression and classification tasks, examples of which are found in [9, 10].

In this analysis we will use a simple GNN to perform classification on single-DOM events. Since the predicted energies of solar-flare neutrinos are too low to apply classification methods that use the large-scale structure of the detector, our aim is to disentangle the neutrino signature from environmental and atmospheric background by looking at coincident hits on a single DOM. This will allow to further expand the energy range probed by KM3NeT to sub-GeV level.

2. Method

The core of this analysis is to perform classification on a small-graph dataset, where our graphs correspond to single-DOM events. These are fixed shape graphs where each node represent one of the 31 PMTs on a DOM, while the edges connect PMTs that are physically close to each other. Most traditional GNN classifiers architecture can be described as a combination of a graph-convolutional model, a readout function, and a multilayer perceptron (MLP). The model that we use for this analysis has been adapted from [11]. This model introduce the hierarchical pooling with structure learning (HGP-SL) operator, which is used to obtain a lower dimensional representation of a graph

preserving the original graph-structure. This algorithm has shown outstanding performances for graph classification on a variety of small-graph benchmark datasets, which have similar features to our MeV-GeV-neutrino dataset.

Our dataset only comprises two classes: the MeV-GeV-neutrino signal, and background. Our signal is made of events built from 0.1-3 GeV muon-neutrino and electron-neutrino simulations, which reproduce the detector response. These simulations were produced using gSeaGen [12] for event generation, and KM3Sim [13] to simulate light propagation in water. The background sample events are instead built using the actual data recorded from the detector in absence of astrophysical transient events. Data was randomly obtained from the KM3NeT/ORCA detector in the period starting on 18 May 2020 at 12:00 and finishing at 18:00 of the same day.

2.1 Single-DOM Events in KM3NeT

2.1.1 Precuts

Precuts have to be applied to L1 data in order to reject the largest portion of background, which is mostly generated by K40 decay coincidences. These cuts also make sure that the classifier avoids training on signal events that are indistinguishable from background. The precuts are performed during the building process of the single-DOM events, i.e., while grouping the coincident hits. For the precuts, the following variables are considered: ToT of individual hits, time offset between hits, and the number of coincident hits in each event. Starting from L1 data and neutrino simulation, we first reject all of the hits with ToT below a threshold. We then look at the hits recorded on the same DOM, and group them in the same event until the time offset between consecutive hits is larger than a maximum time offset. Finally, we discard the events with less than a given number of hits.

In order to optimise these three cuts we study the increments in the fraction of background and signal that is rejected. As there is a clear hierarchy in the impact that these cuts have on the rejected fractions, we investigate them independently. The major rejection is done by constraining the number of hits in the events. The optimal values are found to be:

- Minimum ToT per hit: 6 ns.
- Maximum time offset between hits: 30 ns.
- Minimum number of hits per events: 3.

Roughly 46% of the total (summed) ToT in our simulations survives these cuts, and we have an average event rate of around 56 Hz per DOM in KM3NeT/ORCA at the time period considered for this analysis.

2.1.2 DOM graphs

The graph structured data are processed to naturally reproduce the geometrical configuration of the DOMs. The graphs are thus made of 31 nodes corresponding to the 31 PMTs of a DOM. The edges are drawn between PMTs whose relative distance is smaller than a given threshold. This threshold is chosen to be the smallest value that produces a connected graph for each DOM (with a small margin to account for the inexact cylindrical symmetry of the DOMs). The resulting graphs are shown as processed with NetworkX [14] graphical tools in Fig. 1, together with a representation

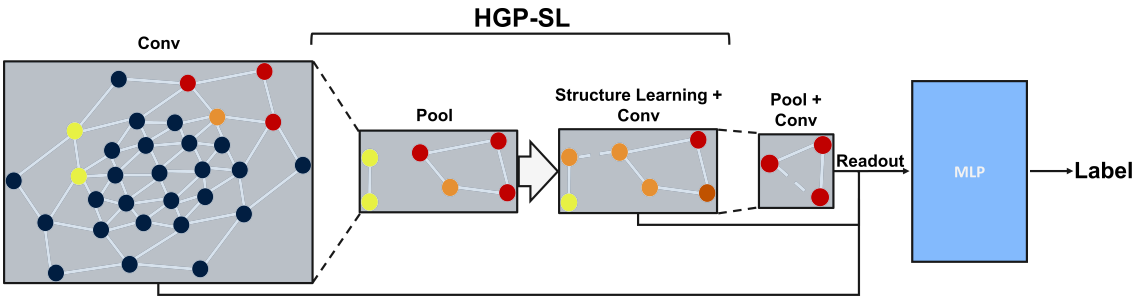

Figure 2: Diagram of the model architecture. Figure inspired by [11].

of the same graph drawn on a DOM. The graphs have a higher density of edges around the nodes that correspond to the lower hemisphere of the DOM, as in this region PMTs are closer together, e.g., in Fig. 1b the node in the centre of the graph represents the lowest PMT on the DOM.

Using full-DOM graphs as opposed to only-hit graphs is fundamental to make our data representative of the spatial distribution of the hits in the events. Each graph is completed by assigning to each node a label corresponding to hit/no-hit, and the measured ToT. When multiple hits occur on the same PMT, in the same event, their ToTs are summed over. Moreover, we compute the standard deviation of the timing of the hits weighted by the corresponding ToT and use it as a graph attribute, this variable describes the spread over time of the deposited charge.

2.2 Model Architecture

For graph classification, we use the model proposed in [11], in the configuration used for classification on the PROTEIN dataset. The original code is provided by the authors and it is publicly available[1]. The model is built on PyTorch [15] and PyTorch Geometric (PyG) [16]. It consists of a series of three Graph Convolutional (GCN) layers, alternated with the hierarchical pooling operator. Starting from the second iteration of convolution and pooling the adjacency matrix of the graph is substituted by the output of the structure learning layer. A readout function is used to combine the output of the three convolutional layers into a vector that is fed into a 3-Layers dense MLP for label-prediction. The full model architecture is shown in Fig. 2. The GCN layers use the GCNConv operator for message-passing, the specifics of which can be found in [17]. This is a common choice for graph convolution, and this layer is readily available in PyG.

The pooling operation is based on the concept of 'information score'. The information score can be interpreted as the distance between the true node representation and the prediction obtained from its neighbours, where a node will receive a lower score if it can be well reconstructed from its neighbours. The idea is that a node with a low score can be removed from the graph without losing much of the information encoded in the original graph. This allows to select the subset of most significative nodes, i.e. with the highest score, for the pooled graph. The number of nodes in the pooled graph is specified by the 'pooling ratio' hyper-parameter. The pooling ratio is defined as the fraction of the number of nodes in the pooled graph and the number of nodes in the graph before pooling. It is set to 0.5 such that graphs halve in size each time pooling is performed.

[1]Code is available at https://github.com/cszhangzhen/HGP-SL

Structure learning is the other main component of the HGP-SL operator. It is used to deal with the problem of the highly-disconnected graphs that can arise from the pooling operation. As the subset of nodes selected during pooling is likely composed of non-neighbouring nodes, this can hinder the effectiveness of the following convolution. This is an artifact of the way that the pooling is performed, but its effect can be mitigated by virtually drawing additional edges in the pooled graph. The main goal of structure learning is to reproduce the structure of the original graph in the pooled graph to allow for better message passing. This is done by creating a substitute to the adjacency matrix, which is obtained by learning an optimal similarity between the nodes of the original graph. The training process is biased to give high similarity to directly connected nodes.

The readout function implemented in this model uses a concatenation of mean pooling and max pooling to obtain an equal-size graph-representation from the outputs of the convolutional layers. The final representation is obtained simply by summing over the individual readouts of the three convolutional layers.

Ultimately, the representation obtained with the readout function is fed into a softmax MLP classifier. This is a linear model made of three dense layers with a pyramidal structure. The number of neurons in the first layer is equal to the readout representation size and double the size of the nodes' hidden representations, which is set to 128. The hidden layer is half the size of the input one, while the output layer is made of two neurons. To train our model we minimize for a cross-entropy loss function over both classes.

2.3 Dataset and training

As mentioned in section 2.1 our dataset is composed of fixed-size graphs with 31 nodes. For this analysis we use a balanced dataset of 1750 events, meaning that half of our graphs have been built from neutrino simulations and labeled as signal, while the other half is built from calibrated

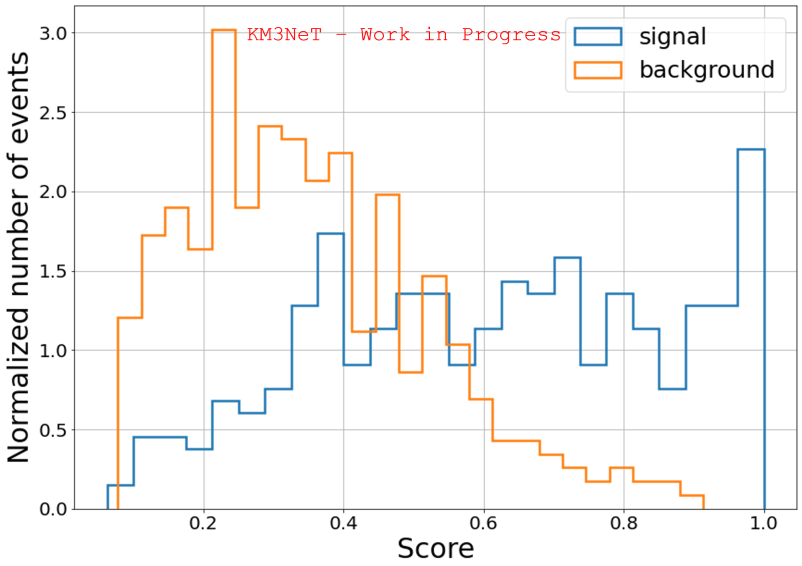

Figure 3: Score distribution of the test sample for the best model on validation. Here signal corresponds to MeV-GeV neutrinos, while background is dominated by environmental noise

L1 data and labeled as background. The reduced size of the dataset is due to the number of neutrino simulations available at the time.

This dataset has been split into three subsets used for training, validation and testing. These subsets correspond respectively to 50%, 10% and 40% of the full sample. this subdivision has been chosen to allow for higher statistics in the testing sample in order to reduce statistical fluctuations in the score distribution shown in Fig. 3.

As per common practice, the model is trained by minimizing a cross-entropy loss function on the training dataset, where at the end of each epoch the model is tested on the validation sample, and training is interrupted when the loss on validation stops decreasing. The best model is chosen to be the one with the lower loss on validation, which implies that 15 more epochs have been tested afterwards without producing better results.

3. Conclusions and prospects

We presented here a method to use KM3NeT for solar-flare neutrino searches in the MeV-GeV energy range. We propose to use single-DOM events to identify the MeV-GeV-neutrino signature enhancing the sensitivity of the detector to low-energies transient sources. By investigating low-level data and neutrino simulations, and implementing hard cuts on the ToT, time coincidence, and number of hits we are able to partially reject atmospheric and environmental background. Starting from the hits that survive these cuts, we build a graph dataset that encodes the information on timing, deposited charge, and geometrical distribution of coincident hits on the same DOM. We conclude our event selection by training a GNN to perform classification on this dataset. Despite the limiting low statistics, preliminary investigations show promising performances.

The single-DOM nature of this selection allows it to be used on both KM3NeT/ORCA, and KM3NeT/ARCA data, making use of the full detector volume. Further investigations will focus on including a high-energy veto using multiple DOMs coincidences, and deriving the sensitivity of KM3NeT to solar-flare neutrinos and other transient events.

References

[1] KM3NeT collaboration, *Letter of intent for KM3NeT 2.0*, *J. Phys. G* **43** (2016) [1601.07459].

[2] KM3NeT collaboration, *Sensitivity for astrophysical neutrino searches with KM3NeT-ORCA*, *PoS* **ICRC2019** (2020) .

[3] KM3NeT collaboration, *KM3NeT Core Collapse Supernovae observation program in standalone and multi-messenger modes*, *PoS* **ICRC2021** (2021) .

[4] G. De Wasseige, *Solar Flare Neutrinos in the Multi-Messenger Era: Flux Calculations and a Search with the IceCube Neutrino observatory*, Ph.D. thesis, Vrije Universiteit Brussel, 2018.

[5] G.E. Kocharov, G.A. Kovaltsov and I.G. Usoskin, *Solar flare neutrinos*, *Nuovo Cim. C* **14** (1991) .

[6] D. Fargion, *Detecting solar neutrino flares and flavors*, *JHEP* **6** (2004) [hep-ph/0312011].

[7] IceCube collaboration, *Search for GeV neutrino emission during intense gamma-ray solar flares with the IceCube Neutrino Observatory*, *Phys. Rev. D* **103** (2021) [2101.00610].

[8] Super-Kamiokande collaboration, *Searching for neutrinos from solar flares across solar cycles 23 and 24 with the Super-Kamiokande detector*, *arXiv preprint* (2022) [2210.12948].

[9] IceCube collaboration, *Graph Neural Networks for low-energy event classification & reconstruction in IceCube*, *JINST* **17** (2022) [2209.03042].

[10] KM3NeT collaboration, *Graph neural networks for reconstruction and classification in KM3NeT*, *JINST* **16** (2021) [2107.13375].

[11] Z. Zhang, J. Bu, M. Ester et al., *Hierarchical graph pooling with structure learning*, *arXiv preprint* (2019) [1911.05954].

[12] KM3NeT collaboration, *gSeaGen: The KM3NeT GENIE-based code for neutrino telescopes*, *Comput. Phys. Commun.* **256** (2020) [2003.14040].

[13] A.G. Tsirigotis, A. Leisos and S.E. Tzamarias, *HOU Reconstruction & Simulation (HOURS): A complete simulation and reconstruction package for very large volume underwater neutrino telescopes*, *Nucl. Instrum. Meth. A* **626-627** (2011) .

[14] A.A. Hagberg, D.A. Schult and P.J. Swart, *Exploring network structure, dynamics, and function using networkx*, *Proceedings of the 7th Python in Science Conference (SciPy 2008)* (2008) .

[15] A. Paszke, S. Gross, F. Massa et al., *Pytorch: An imperative style, high-performance deep learning library*, *Advances in Neural Information Processing Systems 32* (2019) .

[16] M. Fey and J.E. Lenssen, *Fast Graph Representation Learning with PyTorch Geometric*, *ICLR 2019 Workshop on Representation Learning on Graphs and Manifolds* (2019) [1903.02428].

[17] T.N. Kipf and M. Welling, *Semi-Supervised Classification with Graph Convolutional Networks*, *ICLR 2017* (2016) [1609.02907].

PoS(ICRC2023)1294

Full Authors List: The KM3NeT Collaboration

S. Aiello[a], A. Albert[b,bd], S. Alves Garre[c], Z. Aly[d], A. Ambrosone[f,e], F. Ameli[g], M. Andre[h], E. Androutsou[i], M. Anguita[j], L. Aphecetche[k], M. Ardid[l], S. Ardid[l], H. Atmani[m], J. Aublin[n], L. Bailly-Salins[o], Z. Bardačová[q,p], B. Baret[n], A. Bariego-Quintana[c], S. Basegmez du Pree[r], Y. Becherini[n], M. Bendahman[m,n], F. Benfenati[t,s], M. Benhassi[u,e], D. M. Benoit[v], E. Berbee[r], V. Bertin[d], S. Biagi[w], M. Boettcher[x], D. Bonanno[w], J. Boumaaza[m], M. Bouta[y], M. Bouwhuis[r], C. Bozza[z,e], R. M. Bozza[f,e], H.Brânzaş[aa], F. Bretaudeau[k], R. Bruijn[ab,r], J. Brunner[d], R. Bruno[a], E. Buis[ac,r], R. Buompane[u,e], J. Busto[d], B. Caiffi[ad], D. Calvo[c], S. Campion[g,ae], A. Capone[g,ae], F. Carenini[t,s], V. Carretero[c], T. Cartraud[n], P. Castaldi[af,s], V. Cecchini[c], S. Celli[g,ae], L. Cerisy[d], M. Chabab[ag], M. Chadolias[ah], A. Chen[ai], S. Cherubini[aj,w], T. Chiarusi[s], M. Circella[ak], R. Cocimano[w], J. A. B. Coelho[n], A. Coleiro[n], R. Coniglione[w] P. Coyle[d], A. Creusot[n], A. Cruz[al], G. Cuttone[w], R. Dallier[k], Y. Darras[ah], A. De Benedittis[e], B. De Martino[d], G. De Wasseige[bf], V. Decoene[k], R. Del Burgo[e], U. M. Di Cerbo[e], L. S. Di Mauro[w], I. Di Palma[g,ae], A. F. Díaz[j], C. Diaz[j], D. Diego-Tortosa[w], C. Distefano[w], A. Domi[ah], C. Donzaud[n], D. Dornic[d], M. Dörr[am], E. Drakopoulou[i], D. Drouhin[b,bd], R. Dvornický[q], T. Eberl[ah], E. Eckerová[q,p], A. Eddymaoui[m], T. van Eeden[r], M. Eff[n], D. van Eijk[r], I. El Bojaddaini[y], S. El Hedri[n], A. Enzenhöfer[d], J. de Favereau[bf], G. Ferrara[w], M. D. Filipović[an], F. Filippini[t,s], D. Franciotti[w], L. A. Fusco[z,e], J. Gabriel[ao], S. Gagliardini[g], T. Gal[ah], J. García Méndez[l], A. Garcia Soto[c], C. Gatius Oliver[r], N. Geißelbrecht[ah], H. Ghaddari[y], L. Gialanella[e,u], B. K. Gibson[v], E. Giorgio[w], I. Goos[n], D. Goupilliere[o], S. R. Gozzini[c], R. Gracia[ah], K. Graf[ah], C. Guidi[ap,ad], B. Guillon[o], M. Gutiérrez[aq], H. van Haren[ar], A. Heijboer[r], A. Hekalo[am], L. Hennig[ah], J. J. Hernández-Rey[c], F. Huang[d], W. Idrissi Ibnsalih[e], G. Illuminati[s], C. W. James[al], M. de Jong[as,r], P. de Jong[ab,r], B. J. Jung[r], P. Kalaczyński[at,be], O. Kalekin[ah], U. F. Katz[ah], N. R. Khan Chowdhury[c], A. Khatun[q], G. Kistauri[av,au], C. Kopper[ah], A. Kouchner[aw,n], V. Kulikovskiy[ad], R. Kvatadze[av], M. Labalme[o], R. Lahmann[ah], M. Lamoureux[bf], G. Larosa[w], C. Lastoria[d], A. Lazo[c], S. Le Stum[d], G. Lehaut[o], E. Leonora[a], N. Lessing[c], G. Levi[t,s], M. Lindsey Clark[n], F. Longhitano[a], J. Majumdar[r], L. Malerba[ad], F. Mamedov[p], J. Mańczak[c], A. Manfreda[e], M. Marconi[ap,ad], A. Margiotta[t,s], A. Marinelli[e,f], C. Markou[i], L. Martin[k], J. A. Martínez-Mora[l], F. Marzaioli[u,e], M. Mastrodicasa[ae,g], S. Mastroianni[e], J. Mauro[bf], S. Miccichè[w], G. Miele[f,e], P. Migliozzi[e], E. Migneco[w], M. L. Mitsou[e], C. M. Mollo[e], L. Morales-Gallegos[u,e], C. Morley-Wong[al], A. Moussa[y], I. Mozun Mateo[ay,ax], R. Muller[r], M. R. Musone[e,u], M. Musumeci[w], L. Nauta[r], S. Navas[aq], A. Nayerhoda[ak], C. A. Nicolau[g], B. Nkosi[ai], B. Ó Fearraigh[ab,r], V. Oliviero[f,e], A. Orlando[w], E. Oukacha[n], D. Paesani[w], J. Palacios González[c], G. Papalashvili[au], V. Parisi[ap,ad], E.J. Pastor Gomez[c], A. M. Păun[aa], G. E. Păvălaş[aa], S. Peña Martínez[n], M. Perrin-Terrin[d], J. Perronnel[o], V. Pestel[ay], R. Pestes[n], P. Piattelli[w], C. Poirè[z,e], V. Popa[aa], T. Pradier[b], S. Pulvirenti[w], G. Quéméner[o], C. Quiroz[l], U. Rahaman[c], N. Randazzo[a], R. Randriatoamanana[k], S. Razzaque[az], I. C. Rea[e], D. Real[c], S. Reck[ah], G. Riccobene[w], J. Robinson[x], A. Romanov[ap,ad], A. Šaina[c], F. Salesa Greus[c], D. F. E. Samtleben[as,r], A. Sánchez Losa[c,ak], S. Sanfilippo[w], M. Sanguineti[ap,ad], C. Santonastaso[ba,e], D. Santonocito[w], P. Sapienza[w], J. Schnabel[ah], J. Schumann[ah], H. M. Schutte[x], J. Seneca[r], N. Sennan[y], B. Setter[ah], I. Sgura[ak], R. Shanidze[au], Y. Shitov[p], F. Šimkovic[q], A. Simonelli[e], A. Sinopoulou[a], M.V. Smirnov[ah], B. Spisso[e], M. Spurio[t,s], D. Stavropoulos[i], I. Štekl[p], M. Taiuti[ap,ad], Y. Tayalati[m], H. Tedjditi[ad], H. Thiersen[x], I. Tosta e Melo[a,aj], B. Trocmé[n], V. Tsourapis[i], E. Tzamariudaki[i], A. Vacheret[o], V. Valsecchi[w], V. Van Elewyck[aw,n], G. Vannoye[d], G. Vasileiadis[bb], F. Vazquez de Sola[r], C. Verilhac[n], A. Veutro[g,ae], S. Viola[w], D. Vivolo[u,e], J. Wilms[bc], E. de Wolf[ab,r], H. Yepes-Ramirez[l], G. Zarpapis[i], S. Zavatarelli[ad], A. Zegarelli[g,ae], D. Zito[w], J. D. Zornoza[c], J. Zúñiga[c], and N. Zywucka[x].

[a] INFN, Sezione di Catania, Via Santa Sofia 64, Catania, 95123 Italy
[b] Université de Strasbourg, CNRS, IPHC UMR 7178, F-67000 Strasbourg, France
[c] IFIC - Instituto de Física Corpuscular (CSIC - Universitat de València), c/Catedrático José Beltrán, 2, 46980 Paterna, Valencia, Spain
[d] Aix Marseille Univ, CNRS/IN2P3, CPPM, Marseille, France
[e] INFN, Sezione di Napoli, Complesso Universitario di Monte S. Angelo, Via Cintia ed. G, Napoli, 80126 Italy
[f] Università di Napoli "Federico II", Dip. Scienze Fisiche "E. Pancini", Complesso Universitario di Monte S. Angelo, Via Cintia ed. G, Napoli, 80126 Italy
[g] INFN, Sezione di Roma, Piazzale Aldo Moro 2, Roma, 00185 Italy
[h] Universitat Politècnica de Catalunya, Laboratori d'Aplicacions Bioacústiques, Centre Tecnològic de Vilanova i la Geltrú, Avda. Rambla Exposició, s/n, Vilanova i la Geltrú, 08800 Spain
[i] NCSR Demokritos, Institute of Nuclear and Particle Physics, Ag. Paraskevi Attikis, Athens, 15310 Greece
[j] University of Granada, Dept. of Computer Architecture and Technology/CITIC, 18071 Granada, Spain
[k] Subatech, IMT Atlantique, IN2P3-CNRS, Université de Nantes, 4 rue Alfred Kastler - La Chantrerie, Nantes, BP 20722 44307 France
[l] Universitat Politècnica de València, Instituto de Investigación para la Gestión Integrada de las Zonas Costeras, C/ Paranimf, 1, Gandia, 46730 Spain
[m] University Mohammed V in Rabat, Faculty of Sciences, 4 av. Ibn Battouta, B.P. 1014, R.P. 10000 Rabat, Morocco
[n] Université Paris Cité, CNRS, Astroparticule et Cosmologie, F-75013 Paris, France
[o] LPC CAEN, Normandie Univ, ENSICAEN, UNICAEN, CNRS/IN2P3, 6 boulevard Maréchal Juin, Caen, 14050 France
[p] Czech Technical University in Prague, Institute of Experimental and Applied Physics, Husova 240/5, Prague, 110 00 Czech Republic
[q] Comenius University in Bratislava, Department of Nuclear Physics and Biophysics, Mlynska dolina F1, Bratislava, 842 48 Slovak Republic
[r] Nikhef, National Institute for Subatomic Physics, PO Box 41882, Amsterdam, 1009 DB Netherlands
[s] INFN, Sezione di Bologna, v.le C. Berti-Pichat, 6/2, Bologna, 40127 Italy
[t] Università di Bologna, Dipartimento di Fisica e Astronomia, v.le C. Berti-Pichat, 6/2, Bologna, 40127 Italy
[u] Università degli Studi della Campania "Luigi Vanvitelli", Dipartimento di Matematica e Fisica, viale Lincoln 5, Caserta, 81100 Italy
[v] E. A. Milne Centre for Astrophysics, University of Hull, Hull, HU6 7RX, United Kingdom

PoS(ICRC2023)1294

[w] INFN, Laboratori Nazionali del Sud, Via S. Sofia 62, Catania, 95123 Italy
[x] North-West University, Centre for Space Research, Private Bag X6001, Potchefstroom, 2520 South Africa
[y] University Mohammed I, Faculty of Sciences, BV Mohammed VI, B.P. 717, R.P. 60000 Oujda, Morocco
[z] Università di Salerno e INFN Gruppo Collegato di Salerno, Dipartimento di Fisica, Via Giovanni Paolo II 132, Fisciano, 84084 Italy
[aa] ISS, Atomistilor 409, Măgurele, RO-077125 Romania
[ab] University of Amsterdam, Institute of Physics/IHEF, PO Box 94216, Amsterdam, 1090 GE Netherlands
[ac] TNO, Technical Sciences, PO Box 155, Delft, 2600 AD Netherlands
[ad] INFN, Sezione di Genova, Via Dodecaneso 33, Genova, 16146 Italy
[ae] Università La Sapienza, Dipartimento di Fisica, Piazzale Aldo Moro 2, Roma, 00185 Italy
[af] Università di Bologna, Dipartimento di Ingegneria dell'Energia Elettrica e dell'Informazione "Guglielmo Marconi", Via dell'Università 50, Cesena, 47521 Italia
[ag] Cadi Ayyad University, Physics Department, Faculty of Science Semlalia, Av. My Abdellah, P.O.B. 2390, Marrakech, 40000 Morocco
[ah] Friedrich-Alexander-Universität Erlangen-Nürnberg (FAU), Erlangen Centre for Astroparticle Physics, Nikolaus-Fiebiger-Straße 2, 91058 Erlangen, Germany
[ai] University of the Witwatersrand, School of Physics, Private Bag 3, Johannesburg, Wits 2050 South Africa
[aj] Università di Catania, Dipartimento di Fisica e Astronomia "Ettore Majorana", Via Santa Sofia 64, Catania, 95123 Italy
[ak] INFN, Sezione di Bari, via Orabona, 4, Bari, 70125 Italy
[al] International Centre for Radio Astronomy Research, Curtin University, Bentley, WA 6102, Australia
[am] University Würzburg, Emil-Fischer-Straße 31, Würzburg, 97074 Germany
[an] Western Sydney University, School of Computing, Engineering and Mathematics, Locked Bag 1797, Penrith, NSW 2751 Australia
[ao] IN2P3, LPC, Campus des Cézeaux 24, avenue des Landais BP 80026, Aubière Cedex, 63171 France
[ap] Università di Genova, Via Dodecaneso 33, Genova, 16146 Italy
[aq] University of Granada, Dpto. de Física Teórica y del Cosmos & C.A.F.P.E., 18071 Granada, Spain
[ar] NIOZ (Royal Netherlands Institute for Sea Research), PO Box 59, Den Burg, Texel, 1790 AB, the Netherlands
[as] Leiden University, Leiden Institute of Physics, PO Box 9504, Leiden, 2300 RA Netherlands
[at] National Centre for Nuclear Research, 02-093 Warsaw, Poland
[au] Tbilisi State University, Department of Physics, 3, Chavchavadze Ave., Tbilisi, 0179 Georgia
[av] The University of Georgia, Institute of Physics, Kostava str. 77, Tbilisi, 0171 Georgia
[aw] Institut Universitaire de France, 1 rue Descartes, Paris, 75005 France
[ax] IN2P3, 3, Rue Michel-Ange, Paris 16, 75794 France
[ay] LPC, Campus des Cézeaux 24, avenue des Landais BP 80026, Aubière Cedex, 63171 France
[az] University of Johannesburg, Department Physics, PO Box 524, Auckland Park, 2006 South Africa
[ba] Università degli Studi della Campania "Luigi Vanvitelli", CAPACITY, Laboratorio CIRCE - Dip. Di Matematica e Fisica - Viale Carlo III di Borbone 153, San Nicola La Strada, 81020 Italy
[bb] Laboratoire Univers et Particules de Montpellier, Place Eugène Bataillon - CC 72, Montpellier Cédex 05, 34095 France
[bc] Friedrich-Alexander-Universität Erlangen-Nürnberg (FAU), Remeis Sternwarte, Sternwartstraße 7, 96049 Bamberg, Germany
[bd] Université de Haute Alsace, rue des Frères Lumière, 68093 Mulhouse Cedex, France
[be] AstroCeNT, Nicolaus Copernicus Astronomical Center, Polish Academy of Sciences, Rektorska 4, Warsaw, 00-614 Poland
[bf] UCLouvain, Centre for Cosmology, Particle Physics and Phenomenology, Chemin du Cyclotron, 2, Louvain-la-Neuve, 1349 Belgium

Acknowledgements for the KM3NeT Collaboration

The authors acknowledge the financial support of the funding agencies: Agence Nationale de la Recherche (contract ANR-15-CE31-0020), Centre National de la Recherche Scientifique (CNRS), Commission Européenne (FEDER fund and Marie Curie Program), LabEx UnivEarthS (ANR-10-LABX-0023 and ANR-18-IDEX-0001), Paris Île-de-France Region, France; Shota Rustaveli National Science Foundation of Georgia (SRNSFG, FR-22-13708), Georgia; The General Secretariat of Research and Innovation (GSRI), Greece Istituto Nazionale di Fisica Nucleare (INFN), Ministero dell'Università e della Ricerca (MIUR), PRIN 2017 program (Grant NAT-NET 2017W4HA7S) Italy; Ministry of Higher Education, Scientific Research and Innovation, Morocco, and the Arab Fund for Economic and Social Development, Kuwait; Nederlandse organisatie voor Wetenschappelijk Onderzoek (NWO), the Netherlands; The National Science Centre, Poland (2021/41/N/ST2/01177); The grant "AstroCeNT: Particle Astrophysics Science and Technology Centre", carried out within the International Research Agendas programme of the Foundation for Polish Science financed by the European Union under the European Regional Development Fund; National Authority for Scientific Research (ANCS), Romania; Grants PID2021-124591NB-C41, -C42, -C43 funded by MCIN/AEI/ 10.13039/501100011033 and, as appropriate, by "ERDF A way of making Europe", by the "European Union" or by the "European Union NextGenerationEU/PRTR", Programa de Planes Complementarios I+D+I (refs. ASFAE/2022/023, ASFAE/2022/014), Programa Prometeo (PROMETEO/2020/019) and GenT (refs. CIDEGENT/2018/034, /2019/043, /2020/049. /2021/23) of the Generalitat Valenciana, Junta de Andalucía (ref. SOMM17/6104/UGR, P18-FR-5057), EU: MSC program (ref. 101025085), Programa María Zambrano (Spanish Ministry of Universities, funded by the European Union, NextGenerationEU), Spain; The European Union's Horizon 2020 Research and Innovation Programme (ChETEC-INFRA - Project no. 101008324); Fonds de la Recherche Scientifique - FNRS, Belgium.